

Strange hidden-charm tetraquarks in constituent quark models

Xin Jin^{1,*}, Xuejie Liu^{2,†}, Yaoyao Xue^{1,‡}, Hongxia Huang^{1,§} and Jialun Ping^{1,¶}

¹*Department of Physics, Nanjing Normal University, Nanjing 210023, P.R. China and*

²*School of Physics, Southeast University, Nanjing 210094, P. R. China*

Inspired by the newly reported $Z_{cs}(3985)^-$ by the BESIII Collaboration, we systematically investigate the strange hidden-charm tetraquark systems $c\bar{s}\bar{c}u$ with two structures: meson-meson and diquark-antidiquark. Two quark models: the chiral quark model (ChQM) and the quark delocalization color screening model (QDCSM) are used here. Similar results are obtained in both two quark models. There is no any bound state in either ChQM or QDCSM, which excludes the molecular state explanation ($D_s D^*/D_s^* D/D_s^* D^*$) of the reported $Z_{cs}(3985)^-$. However, the effective potentials for the diquark-antidiquark $c\bar{s}\bar{c}u$ systems shows the possibility of some resonance states with mass range of $3916.5 \sim 3964.6$ MeV for $IJ^P = \frac{1}{2}0^+$, $4008.8 \sim 4091.2$ MeV for $IJ^P = \frac{1}{2}1^+$, $4246.8 \sim 4418.1$ MeV for $IJ^P = \frac{1}{2}2^+$. So the observed $Z_{cs}(3985)^-$ state is possible to be explained as a compact resonance state composed of $c\bar{s}\bar{c}u$ with $IJ^P = \frac{1}{2}0^+$ or $IJ^P = \frac{1}{2}1^+$. The study of the scattering process of corresponding open channels is under way to check this conclusion.

PACS numbers: 13.75.Cs, 12.39.Pn, 12.39.Jh

I. INTRODUCTION

In 2013, the BESIII Collaboration studied the $e^+e^- \rightarrow J/\psi\pi^+\pi^-$ process at a center-of-mass energy of 4.26 GeV and reported a new charged charmonium-like structure in the $\pi^\pm J/\psi$ invariant spectrum, which is called $Z_c(3900)$ and has a mass of $3899.0 \pm 3.6 \pm 4.9$ MeV and a width of $46 \pm 10 \pm 20$ MeV [1]. At the same time, the Belle observed a $Z_c(3895)^\pm$ state, with a mass of $3894.5 \pm 6.6 \pm 4.5$ MeV and a width of $63 \pm 24 \pm 26$ MeV in the process $Y(4260) \rightarrow J/\psi\pi^+\pi^-$ [2]. The mass and width of $Z_c(3900)$ and $Z_c(3895)^\pm$ are very close within errors, so they are the same state [3]. The state $Z_c(3900)$ has been further confirmed by the CLEO-c Collaboration in the decay $Y(4160) \rightarrow J/\psi\pi^+\pi^-$ [4]. Subsequently, there is a lot of theoretical work to study $Z_c(3900)$ and its associated states. Some researches treated it as the tightly bound diquark-antidiquark state [5–10]. However, many researches treated it as molecular states [11–17]. Some indicated that the $Z_c(3900)$ is not a usual resonance but a threshold cusp [18, 19]. Lattice QCD method is also used to find $Z_c(3900)$, but it has not been found [20–23].

Very recently, the BESIII Collaboration reported their study of the processes of $e^+e^- \rightarrow K^+(D_s^- D^{*0} + D_s^{*-} D^0)$, and found a new structure $Z_{cs}(3985)^-$ near the $D_s^- D^{*0}/D_s^{*-} D^0$ thresholds in the K^+ recoil-mass spectrum for events collected at $\sqrt{s} = 4.681$ GeV. The pole mass and width of this state are $(3982.5_{-2.6}^{+1.8} \pm 2.1)$ MeV and $(12.8_{-4.4}^{+5.3} \pm 3.0)$ MeV, respectively [24]. From the production mode, it is easy to get that the minimum quark component of $Z_{cs}(3985)^-$ is $c\bar{c}s\bar{q}$ ($q = u/d$),

and this state should be a partner structure of the well-known $Z_c(3885)^-$ reported in $e^+e^- \rightarrow D^{*-} D^0 \pi^+$ [25]. Besides, it is the first candidate of the charged hidden-charm tetraquark state with strangeness, whose discovery can provide more hints to the quest of charged exotic Z structures. Therefore, the observation of $Z_{cs}(3985)^-$ immediately stimulated a lot of theoretical discussions [26–35].

Actually, theoretical predictions of the charged hidden-charm tetraquark with strangeness have been made in different models [36–38]. D.Ebert used relativistic quark model based on the quasipotential approach to calculate the mass spectra of tetraquarks $[Qs][\bar{Q}\bar{q}]/[Qq][\bar{Q}\bar{s}]$ ($Q = c, b$) [39]. They found that all S -wave tetraquarks with hidden bottom lie considerably below open bottom thresholds and they should be narrow states which can be observed experimentally. However hidden-charm tetraquark states all above open charm thresholds. Di- anyong Chen indicated that there exist enhancement structures with both hidden-charm and open-strange decays, which are near the $D\bar{D}_s^*/D^*\bar{D}_s$ and $D^*\bar{D}_s^*/\bar{D}^*D_s^*$ thresholds under the initial single chiral particle emission (ISChE) mechanism [40]. Chengrong Deng studied the same charged tetraquark states using the variational method GEM in the color flux-tube model with a four-body confinement potential. The numerical results indicated that some compact resonance states can be formed [7].

Strong interaction is the strongest of the four interactions in nature, but understanding its nature has always been a difficult problem in physics. Quantum chromodynamics (QCD) is widely accepted as the basic theory of strong interactions. QCD can deal with scattering problems by perturbation expansion in high energy regions, but the spontaneous chiral symmetry breaking and color confinement appear in low energy regions. To study hadron-hadron interactions and multiquark states, many quark models based on QCD theory have been developed. The chiral quark model (ChQM) is one of the

*E-mail: 181002005@stu.njnu.edu.cn

†E-mail: 1830592517@qq.com

‡E-mail: 181002022@stu.njnu.edu.cn

§E-mail: hxhuang@njnu.edu.cn (Corresponding author)

¶E-mail: jlping@njnu.edu.cn (Corresponding author)

accepted models [41]. The interactions in this model include the colorful one-gluon-exchange and confinement, colorless Goldstone boson exchange and the chiral partner σ meson-exchange. Another approach is the quark delocalization color screening model (QDCSM), which was developed to study the similarities between nuclear and molecular forces [42]. Both of these two models describe the properties of deuteron, nucleon-nucleon and hyperon-nucleon interactions well [43, 44]. Very recently, both ChQM and QDCSM have been used to explain the full-heavy tetraquark states [45] and the reported $X(6900)$ by LHCb collaboration [46] could be explained as a compact resonance state in both two models. It is quite natural to extend the study to the charged hidden-charm tetraquark systems with strangeness. So we investigate the tetraquark systems composed of $c\bar{c}s\bar{q}$ ($q = u/d$) in both ChQM and QDCSM in present work.

The structure of this paper is as follows. section II gives a brief introduction of two quark models, and the construction of wave functions. The numerical results and discussions are given in Section III. The summary is presented in the last section.

II. MODELS AND WAVEFUNCTIONS

In this work, we investigate the charged charmonium-like tetraquarks with hidden-charm and open-strange $c\bar{c}s\bar{q}$ ($q = u/d$) within two quark models: ChQM and QDCSM. Two structures: meson-meson and diquark-antidiquark, are considered. In this sector, we will introduce these two models and the wave functions of the tetraquarks for two structures.

A. The chiral quark model (ChQM)

The ChQM has been successfully applied to describe the properties of hadrons and hadron-hadron interactions [41, 47]. The model details can be found in Ref. [41, 47]. We only show the Hamiltonian of the model here.

$$H = \sum_{i=1}^4 \left(m_i + \frac{p_i^2}{2m_i} \right) - T_{cm} + \sum_{i=1 < j}^4 (V_{ij}^{CON} + V_{ij}^{OGE}) \quad (1)$$

where T_{cm} is the kinetic energy of the center of mass; V_{ij}^{CON} and V_{ij}^{OGE} are the interactions of the confinement and the one-gluon-exchange, respectively. For the $c\bar{c}s\bar{u}$ system, there is no σ -exchange interactions, because the σ meson cannot be exchanged between u/d quark and s/c quark. The forms of V_{ij}^{CON} and V_{ij}^{OGE} are shown

below:

$$V_{ij}^{CON} = -\lambda_i^c \cdot \lambda_j^c (a_c r_{ij}^2 + V_{0ij}) \quad (2)$$

$$V_{ij}^{OGE} = \frac{\alpha_{s_{ij}}}{4} \lambda_i^c \cdot \lambda_j^c \left[\frac{1}{r_{ij}} - \frac{\pi}{2} \delta(\mathbf{r}_{ij}) \left(\frac{1}{m_i^2} + \frac{1}{m_j^2} + \frac{4\boldsymbol{\sigma}_i \cdot \boldsymbol{\sigma}_j}{3m_i m_j} \right) - \frac{3}{4m_i m_j r_{ij}^3} S_{ij} \right] \quad (3)$$

$$S_{ij} = \left\{ 3 \frac{(\boldsymbol{\sigma}_i \cdot \mathbf{r}_{ij})(\boldsymbol{\sigma}_j \cdot \mathbf{r}_{ij})}{r_{ij}^2} - \boldsymbol{\sigma}_i \cdot \boldsymbol{\sigma}_j \right\} \quad (4)$$

where S_{ij} is quark tensor operator; $\alpha_{s_{ij}}$ is the quark-gluon coupling constant.

B. The quark delocalization color screening model (QDCSM)

Generally, the Hamiltonian of QDCSM is almost the same as that of ChQM, but with two modifications [42]. The one is that there is no σ -meson exchange in QDCSM, and another one is that the screened color confinement is used between quark pairs reside in different clusters, aiming to take into account the QCD effect which has not yet been included in the two-body confinement. The confining potential in QDCSM was modified as follows:

$$V_{ij}^{CON} = \begin{cases} -\lambda_i^c \cdot \lambda_j^c (a_c r_{ij}^2 + V_{0ij}) & \text{i, j in the same cluster} \\ -\lambda_i^c \cdot \lambda_j^c a_c \frac{1 - e^{-\mu_{ij} r_{ij}^2}}{\mu_{ij}} & \text{, otherwise} \end{cases}$$

where μ_{ij} is the color screening parameter, which is determined by fitting the deuteron properties, NN scattering phase shifts, and $N\Lambda$ and $N\Sigma$ scattering phase shifts, respectively, with $\mu_{uu} = 0.45 \text{ fm}^{-2}$, $\mu_{us} = 0.19 \text{ fm}^{-2}$ and $\mu_{ss} = 0.08 \text{ fm}^{-2}$, satisfying the relation, $\mu_{us}^2 = \mu_{uu}\mu_{ss} = 0.19 \text{ fm}^{-2}$ [44]. When extending to the heavy quark case, there is no experimental data available, so we take it as a adjustable parameter $\mu_{cc} = 0.01 \sim 0.001 \text{ fm}^{-2}$ and we find the results are insensitive to the value of μ_{cc} . So in the present work, we take $\mu_{cc} = 0.01 \text{ fm}^{-2}$, $\mu_{uc} = 0.067 \text{ fm}^{-2}$ and $\mu_{sc} = 0.0283 \text{ fm}^{-2}$.

The single particle orbital wave functions in the ordinary quark cluster model are the left and right centered single Gaussian functions:

$$\begin{aligned} \phi_\alpha(\mathbf{S}_i) &= \left(\frac{1}{\pi b^2} \right)^{\frac{3}{4}} e^{-\frac{(\mathbf{r} - \mathbf{S}_i/2)^2}{2b^2}}, \\ \phi_\beta(-\mathbf{S}_i) &= \left(\frac{1}{\pi b^2} \right)^{\frac{3}{4}} e^{-\frac{(\mathbf{r} + \mathbf{S}_i/2)^2}{2b^2}}. \end{aligned} \quad (5)$$

The quark delocalization in QDCSM is realized by writing the single particle orbital wave function as a linear combination of the left and right Gaussians:

$$\begin{aligned} \psi_\alpha(\mathbf{S}_i, \epsilon) &= (\phi_\alpha(\mathbf{S}_i) + \epsilon \phi_\alpha(-\mathbf{S}_i)) / N(\epsilon), \\ \psi_\beta(-\mathbf{S}_i, \epsilon) &= (\phi_\beta(-\mathbf{S}_i) + \epsilon \phi_\beta(\mathbf{S}_i)) / N(\epsilon), \\ N(\epsilon) &= \sqrt{1 + \epsilon^2 + 2\epsilon e^{-S_i^2/4b^2}}. \end{aligned} \quad (6)$$

where $\epsilon(\mathbf{S}_i)$ is the delocalization parameter determined by the dynamics of the quark system rather than adjusted parameters. In this way, the system can choose its most favorable configuration through its own dynamics in a larger Hilbert space.

The parameters used in our previous work are determined by fitting the mass spectrum of mesons and baryons including light quarks (u , d , s), but the mesons composed of heavy quarks like $\eta_b(\eta_c)$ or $\Upsilon(J/\psi)$ do not fit well. To give the right mass of the mesons we used in this work, we adjust the parameters by fitting the masses of mesons that we need. Since there is no σ -exchange interactions in ChQM for the $c\bar{c}s\bar{u}$ system and the delocalization and color screening in QDCSM work in quarks of different clusters, there is no discrepancy of these two models in describing mesons. So the parameters of two quark models are the same, which are shown in Table I. The calculated masses of the mesons are shown in Table II.

TABLE I: Model parameters.

State	b (fm)	0.3
m_u (MeV)		313
m_s (MeV)		536
m_c (MeV)		1728
Confinement a_c (MeV fm ⁻²)		101
V_{us} (MeV)		-180.6
V_{uc} (MeV)		-133.6
V_{sc} (MeV)		-68.1
V_{cc} (MeV)		76
OGE	α_{sus}	0.33
	α_{suc}	0.38
	α_{suc}	0.66
	α_{suc}	1.67

TABLE II: The calculated masses (in MeV) of the mesons. Experimental values are taken from the Particle Data Group(PDG).

	K	K*	η_c	J/ψ	D	D*	D_s	D_s^*
Exp.	494	892	2984	3097	1865	2007	1968	2112
Model	495	892	2984	3097	1865	2007	1968	2112

C. The wave function

In this work, we study a bound-state problem by a well-established method, the resonating group method (RGM) [48]. In order to calculate the energy of the $c\bar{c}s\bar{u}$ system, we first constructed the four-quark wave function in the following form:

$$\Psi = \mathcal{A}[\psi^L \chi^\sigma]_{JM} \chi^f \chi^c. \quad (7)$$

where ψ^L , χ^σ , χ^f and χ^c are the orbital, spin, flavor and color wave functions, respectively, which are given below. The symbol \mathcal{A} is the anti-symmetrization operator. For the $c\bar{c}s\bar{u}$ system, $\mathcal{A} = 1$ because the quarks are not identical particles in the $SU(3)$ symmetry and no anti-symmetrization requirement is needed here.

1. The orbital wave function

The total orbital wave function is composed of two internal cluster orbital wave functions ($\psi_1(\mathbf{R}_1)$ and $\psi_2(\mathbf{R}_2)$), and one relative motion wave function ($\chi_L(\mathbf{R})$) between two clusters.

$$\psi^L = \psi_1(\mathbf{R}_1)\psi_2(\mathbf{R}_2)\chi_L(\mathbf{R}) \quad (8)$$

where \mathbf{R}_1 and \mathbf{R}_2 are the internal coordinates for the cluster 1 and cluster 2, respectively. $\mathbf{R} = \mathbf{R}_1 - \mathbf{R}_2$ is the relative coordinate between the two clusters 1 and 2. $\chi_L(\mathbf{R})$ is expanded by gaussian bases

$$\chi_L(\mathbf{R}) = \frac{1}{\sqrt{4\pi}} \left(\frac{3}{2\pi b^2} \right) \sum_{i=1}^n C_i \times \int \exp\left[-\frac{3}{4b^2}(\mathbf{R} - \mathbf{s}_i)^2\right] Y_{LM}(\hat{s}_i) d\hat{s}_i \quad (9)$$

where \mathbf{s}_i is the generate coordinate, n is the number of the gaussian bases, which is determined by the stability of the results. By doing this is expansion, we can simplify the integro-differential equation to an algebraic equation, solve this generalized eigen-equation to get the energy of the system more easily. The details of solving the RGM equation can be found in Ref [48].

2. The flavor wave function

The flavor wave function for the $c\bar{c}s\bar{u}$ system is very simple. For the meson-meson structure,

$$\chi_m^{f1} = [c\bar{c}][s\bar{u}] \quad (10)$$

$$\chi_m^{f2} = [c\bar{u}][s\bar{c}] \quad (11)$$

where the superscript of the χ is the index of the flavor wave function for meson-meson structure, and the subscript stands for the isospin I and the third component I_z .

For the diquark-antidiquark structure,

$$\chi_d^{f1} = c\bar{s}\bar{c}\bar{u} \quad (12)$$

The upper and lower indices are similar to those of the meson-meson structure.

3. The spin wave function

For the spin part, the wave functions for two-body clusters are:

$$\begin{aligned} \chi_{\sigma 11}^1 &= \alpha\alpha & \chi_{\sigma 10}^2 &= \sqrt{\frac{1}{2}}(\alpha\beta + \beta\alpha) \\ \chi_{\sigma 1-1}^3 &= \beta\beta & \chi_{\sigma 00}^4 &= \sqrt{\frac{1}{2}}(\alpha\beta - \beta\alpha) \end{aligned} \quad (13)$$

Then, the total spin wave functions for the four-quark system can be obtained by coupling the wave functions of two clusters.

$$\begin{aligned} \chi_{00}^{\sigma 1} &= \chi_{\sigma 00}^4 \chi_{\sigma 00}^4 \\ \chi_{00}^{\sigma 2} &= \sqrt{\frac{1}{3}}(\chi_{\sigma 11}^1 \chi_{\sigma 1-1}^3 - \chi_{\sigma 10}^2 \chi_{\sigma 10}^2 + \chi_{\sigma 1-1}^3 \chi_{\sigma 10}^1) \\ \chi_{11}^{\sigma 3} &= \chi_{\sigma 00}^4 \chi_{\sigma 11}^1 \\ \chi_{11}^{\sigma 4} &= \chi_{\sigma 11}^1 \chi_{\sigma 00}^4 \\ \chi_{11}^{\sigma 5} &= \sqrt{\frac{1}{2}}(\chi_{\sigma 11}^1 \chi_{\sigma 10}^2 - \chi_{\sigma 10}^2 \chi_{\sigma 11}^1) \\ \chi_{22}^{\sigma 6} &= \chi_{\sigma 11}^1 \chi_{\sigma 11}^1 \end{aligned} \quad (14)$$

The spin wave function of two structures is the same.

4. The color wave function

For the meson-meson structure, we give the wave functions for the two-body clusters first, which are

$$\chi_{c[111]}^1 = \sqrt{\frac{1}{3}}(r\bar{r} + g\bar{g} + b\bar{b}) \quad (15)$$

$$\chi_{c[21]}^2 = r\bar{b} \quad \chi_{c[21]}^3 = -r\bar{g}$$

$$\chi_{c[21]}^4 = g\bar{b} \quad \chi_{c[21]}^5 = -b\bar{g}$$

$$\chi_{c[21]}^6 = g\bar{r} \quad \chi_{c[21]}^7 = b\bar{r}$$

$$\chi_{c[21]}^8 = \sqrt{\frac{1}{2}}(r\bar{r} - g\bar{g})$$

$$\chi_{c[21]}^9 = \sqrt{\frac{1}{6}}(-r\bar{r} - g\bar{g} + 2b\bar{b}) \quad (16)$$

where the subscript [111] and [21] stand for the color singlet and color octet cluster respectively.

Then, the total color wave functions for the four-quark system with the meson-meson structure can be obtained

by coupling the wave functions of two clusters.

$$\chi_m^{c1} = \chi_{c[111]}^1 \chi_{c[111]}^1 \quad (17)$$

$$\begin{aligned} \chi_m^{c2} &= \sqrt{\frac{1}{8}}(\chi_{c[21]}^2 \chi_{c[21]}^7 - \chi_{c[21]}^4 \chi_{c[21]}^5 - \chi_{c[21]}^3 \chi_{c[21]}^6 \\ &\quad + \chi_{c[21]}^8 \chi_{c[21]}^8 - \chi_{c[21]}^6 \chi_{c[21]}^3 + \chi_{c[21]}^9 \chi_{c[21]}^9 \\ &\quad - \chi_{c[21]}^5 \chi_{c[21]}^4 + \chi_{c[21]}^7 \chi_{c[21]}^2) \end{aligned} \quad (18)$$

where χ_m^{c1} and χ_m^{c2} represent the color wave function for the color-singlet channel (1×1) and the hidden-color channel (8×8), respectively.

For the diquark-antidiquark structure, we firstly give the color wave functions of the diquark clusters,

$$\begin{aligned} \chi_{c[2]}^1 &= rr & \chi_{c[2]}^2 &= \sqrt{\frac{1}{2}}(rg + gr) & \chi_{c[2]}^3 &= gg \\ \chi_{c[2]}^4 &= \sqrt{\frac{1}{2}}(rb + br) & \chi_{c[2]}^5 &= \sqrt{\frac{1}{2}}(gb + bg) \\ \chi_{c[2]}^6 &= bb & \chi_{c[11]}^7 &= \sqrt{\frac{1}{2}}(rg - gr) \\ \chi_{c[11]}^8 &= \sqrt{\frac{1}{2}}(rb - br) & \chi_{c[11]}^9 &= \sqrt{\frac{1}{2}}(gb - bg) \end{aligned} \quad (19)$$

and the color wave functions of the antidiquark clusters,

$$\begin{aligned} \chi_{c[22]}^1 &= \bar{r}\bar{r} & \chi_{c[22]}^2 &= \sqrt{\frac{1}{2}}(\bar{r}\bar{g} + \bar{g}\bar{r}) & \chi_{c[22]}^3 &= \bar{g}\bar{g} \\ \chi_{c[22]}^4 &= \sqrt{\frac{1}{2}}(\bar{r}\bar{b} + \bar{b}\bar{r}) & \chi_{c[22]}^5 &= \sqrt{\frac{1}{2}}(\bar{g}\bar{b} + \bar{b}\bar{g}) \\ \chi_{c[22]}^6 &= \bar{b}\bar{b} & \chi_{c[211]}^7 &= \sqrt{\frac{1}{2}}(\bar{r}\bar{g} - \bar{g}\bar{r}) \\ \chi_{c[211]}^8 &= \sqrt{\frac{1}{2}}(\bar{r}\bar{b} - \bar{b}\bar{r}) & \chi_{c[211]}^9 &= \sqrt{\frac{1}{2}}(\bar{g}\bar{b} - \bar{b}\bar{g}) \end{aligned} \quad (20)$$

After that, the total wave functions for the four-quark system with the diquark-antidiquark structure are obtained as below,

$$\begin{aligned} \chi_d^{c1} &= \sqrt{\frac{1}{6}}[\chi_{c[2]}^1 \chi_{c[22]}^1 - \chi_{c[2]}^2 \chi_{c[22]}^2 + \chi_{c[2]}^3 \chi_{c[22]}^3 \\ &\quad + \chi_{c[2]}^4 \chi_{c[22]}^4 - \chi_{c[2]}^5 \chi_{c[22]}^5 + \chi_{c[2]}^6 \chi_{c[22]}^6] \end{aligned} \quad (21)$$

$$\chi_d^{c2} = \sqrt{\frac{1}{3}}[\chi_{c[11]}^7 \chi_{c[211]}^7 - \chi_{c[11]}^8 \chi_{c[211]}^8 + \chi_{c[11]}^9 \chi_{c[211]}^9] \quad (22)$$

Finally, we can acquire the total wave functions by substituting the wave functions of the orbital, the spin, the flavor and the color parts into the Eq.(7) according to the given quantum number of the system.

III. NUMERICAL RESULTS AND DISCUSSIONS

In this work, we investigate the charged hidden-charm tetraquark systems with strangeness in two structures,

meson-meson and diquark-antidiquark. We take into account all the possible quantum numbers for the S -wave $c\bar{c}s\bar{u}$ systems, which are $IJ^P = \frac{1}{2}0^+, \frac{1}{2}1^+, \text{ and } \frac{1}{2}2^+$. For the meson-meson structure, we take into account of two color configurations which are the color singlet-singlet (1×1) and color octet-octet (8×8) configurations in the ChQM, while in the QDCSM, we only consider the color singlet-singlet (1×1) configuration, since this model considers the effect of the hidden color channel coupling to some extent [49]. For the diquark-antidiquark structure, two color configurations, antitriplet-triplet ($\bar{3} \times 3$) and sextet-antisextet ($6 \times \bar{6}$), are considered in both models.

To find any bound states of the $c\bar{c}s\bar{u}$ systems, we carry out a dynamical bound-state calculation. The energies of both the single channel and the channel-coupling calculations are obtained. Table III shows the results of the meson-meson structure, and Table IV shows the results of the diquark-antidiquark structure. In the tables, the column headed with $[\chi^{\sigma_i} \chi^{f_j} \chi^{c_k}]$ denotes the combination in spin, flavor and color degrees of freedom for each channel, respectively. The columns headed with E_{th} denotes the theoretical threshold of each channel and E_{sc} represents the lowest energies in the single channel calculation. For meson-meson structure, the column "Channel" represents the physical contents of the channel. The tetraquarks composed of $c\bar{c}s\bar{u}$ can be combined in two ways: $[c\bar{c}][s\bar{u}]$ and $[c\bar{u}][s\bar{c}]$. In each combination, E_{cc1} and E_{cc2} denote the lowest energies of the coupling of the color-singlet channels and the coupling of all channels (including color-singlet channels and hidden-color channels). The coupling of the two combinations is shown in E_{cc3} . For diquark-antidiquark structure, E_{cc1} and E_{cc2} denote the lowest energies of the coupling of the $6 \times \bar{6}$ color configuration and the coupling of all channels (including $6 \times \bar{6}$ and $\bar{3} \times 3$ color configurations). All the general features of the calculated results are as follows.

A. Meson-meson structure

For the meson-meson structure, $\eta_c K$ and $\eta_{c8} K_8$ in Table III represent the color singlet-singlet (1×1) and color octet-octet (8×8) configurations, respectively. From Table III we can see that the energies of every single channel are above the corresponding theoretical threshold in both two models. The channel-coupling calculation cannot help too much, and the energies by the channel-coupling are still above the theoretical threshold, which indicates that the effect of the channel-coupling is very small here. This is mainly due to the large energy difference between each single channel. As a result, in the meson-meson structure, there is no any bound states in either ChQM or QDCSM. So the reported $Z_{cs}(3985)^-$ cannot be explained as $D_s D^* / D_s^* D / D_s^* D^*$ molecular state in present calculation.

To study the interaction between two mesons, we carry out the adiabatic calculation of the effective potentials for

the $c\bar{c}s\bar{u}$ system. For the color singlet channels, the effective potentials in both two quark models are shown in Fig. 1 and Fig. 2, respectively. In ChQM, all effective potentials are repulsive, and that's why we cannot get any bound state. In QDCSM, although the effective potential of every channel is attractive, it is not strong enough to form any bound state. For the hidden color channel, we only gives the potential of ChQM in Fig. 3, because the effect of the hidden color channel coupling is considered to some extent in QDCSM. From Fig. 3 we can see that the minimum potential of each channel appears at the separation of 0.3 or 0.4 fm, which indicates that two colorful subclusters are not willing to huddle together or fall apart, so it is possible to form some resonance states here. However, the energy of the hidden color channel listed in Table III is among $4.1 \sim 4.6$ GeV, which indicates that these resonances may not be suitable to explain the observed $Z_{cs}(3985)^-$. The scattering process of the corresponding open channels should be studied to confirm if there is any resonance state or not.

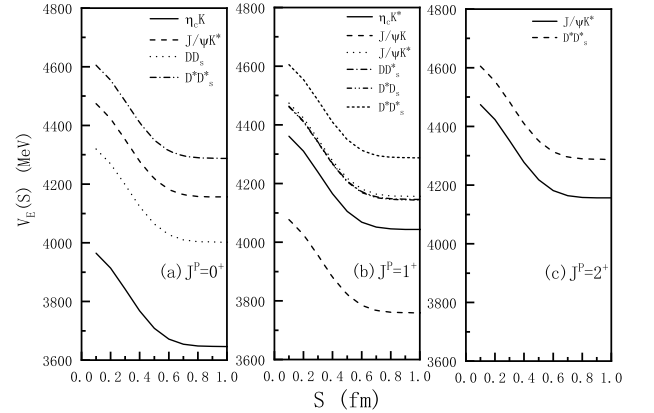


FIG. 1: The effective potentials of the color singlet channels for the meson-meson $c\bar{c}s\bar{u}$ systems in ChQM.

We also try to investigate why the effective potentials of the two models are different in the color singlet channels. The Hamiltonian of the ChQM and the QDCSM consists of mass, the kinetic energy (V_{VK}), the confinement (V_{CON}), the Coulomb interaction (V_{Coul}) and the color-magnetic interaction (V_{CMI}). We take the results of the $IJ^P = \frac{1}{2}0^+ \eta_c K$ channel in meson-meson structure as an example in Fig. 4. We can see that the kinetic energy term in the ChQM provides repulsion, while the one in QDCSM provides attractive interactions. In the ChQM, the confinement (V_{CON}), the Coulomb interaction (V_{Coul}) and the color-magnetic interaction (V_{CMI}) do not contribute to the effective potential between two color singlet clusters $c\bar{c}$ and $s\bar{u}$, so the interaction between the two mesons is only affected by the kinetic energy term (V_{VK}). There is no exchange terms between $c\bar{c}$ and $s\bar{u}$ in ChQM, so the confinement interaction, the Coulomb interaction and the color-magnetic interaction

TABLE III: The energies (in MeV) of $c\bar{c}s\bar{u}$ systems with the meson-meson structure in the ChQM and QDCSM.

			ChQM					QDCSM		
IJ^P	$[\chi^{\sigma_i} \chi^{f_j} \chi^{c_k}]$	Channel	E_{th}	E_{sc}	E_{cc1}	E_{cc2}	E_{cc3}	E_{sc}	E_{cc1}	E_{cc3}
$\frac{1}{2}0^+$	$\chi_{00}^{\sigma1} \chi_m^{f1} \chi_m^{c1}$	$\eta_c K$	3478.2	3484.9	3484.9	3484.9	3484.9	3484.9	3484.9	3484.9
	$\chi_{00}^{\sigma2} \chi_m^{f1} \chi_m^{c1}$	$J/\psi K^*$	3988.1	3994.8				3994.1		
	$\chi_{00}^{\sigma1} \chi_m^{f1} \chi_m^{c2}$	$\eta_{c8} K_8$		4542.6						
	$\chi_{00}^{\sigma2} \chi_m^{f1} \chi_m^{c2}$	$J/\psi_8 K_8^*$		4363.8						
	$\chi_{00}^{\sigma1} \chi_m^{f2} \chi_m^{c1}$	DD_s	3833.4	3840.6	3840.6	3838.3		3840.1	3840.1	
	$\chi_{00}^{\sigma2} \chi_m^{f2} \chi_m^{c1}$	$D^* D_s^*$	4119.5	4126.2				4121.2		
	$\chi_{00}^{\sigma1} \chi_m^{f2} \chi_m^{c2}$	$D_8 D_{s8}$		4395.5						
	$\chi_{00}^{\sigma2} \chi_m^{f2} \chi_m^{c2}$	$D_8^* D_{s8}^*$		4125.3						
$\frac{1}{2}1^+$	$\chi_{11}^{\sigma3} \chi_m^{f1} \chi_m^{c1}$	$\eta_c K^*$	3875.2	3881.9	3597.8	3597.8	3597.8	3881.6	3597.8	3597.7
	$\chi_{11}^{\sigma4} \chi_m^{f1} \chi_m^{c1}$	$J/\psi K$	3591.1	3597.8				3597.8		
	$\chi_{11}^{\sigma5} \chi_m^{f1} \chi_m^{c1}$	$J/\psi K^*$	3988.1	3994.8				3994.1		
	$\chi_{11}^{\sigma3} \chi_m^{f1} \chi_m^{c2}$	$\eta_{c8} K_8^*$		4493.0						
	$\chi_{11}^{\sigma4} \chi_m^{f1} \chi_m^{c2}$	$J/\psi_8 K_8$		4528.5						
	$\chi_{11}^{\sigma5} \chi_m^{f1} \chi_m^{c2}$	$J/\psi_8 K_8^*$		4423.6						
	$\chi_{11}^{\sigma3} \chi_m^{f2} \chi_m^{c1}$	DD_s^*	3977.7	3984.4	3982.4	3980.2		3983.1	3981.1	
	$\chi_{11}^{\sigma4} \chi_m^{f2} \chi_m^{c1}$	$D^* D_s$	3975.7	3982.4				3981.1		
	$\chi_{11}^{\sigma5} \chi_m^{f2} \chi_m^{c1}$	$D^* D_s^*$	4119.5	4126.2				4121.2		
	$\chi_{11}^{\sigma3} \chi_m^{f2} \chi_m^{c2}$	$D_8 D_{s8}^*$		4377.5						
	$\chi_{11}^{\sigma4} \chi_m^{f2} \chi_m^{c2}$	$D_8^* D_{s8}$		4377.7						
	$\chi_{11}^{\sigma5} \chi_m^{f2} \chi_m^{c2}$	$D_8^* D_{s8}^*$		4247.2						
$\frac{1}{2}2^+$	$\chi_{11}^{\sigma6} \chi_m^{f1} \chi_m^{c1}$	$J/\psi K^*$	3988.1	3994.8		3994.8	3994.8	3994.1		3994.1
	$\chi_{11}^{\sigma6} \chi_m^{f1} \chi_m^{c2}$	$J/\psi_8 K_8^*$		4529.6						
	$\chi_{11}^{\sigma6} \chi_m^{f2} \chi_m^{c1}$	$D^* D_s^*$	4119.5	4126.2		4124.0		4121.2		
	$\chi_{11}^{\sigma6} \chi_m^{f2} \chi_m^{c2}$	$D_8^* D_{s8}^*$		4462.0						

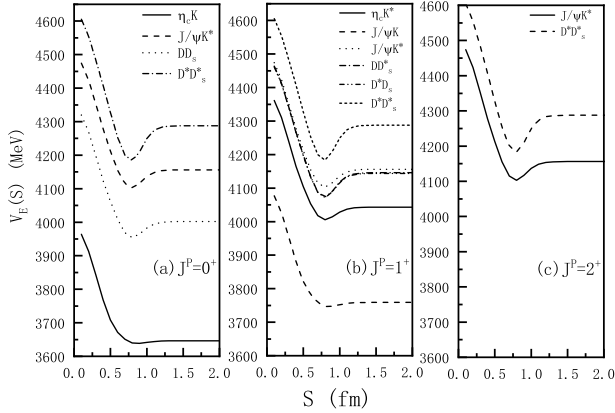
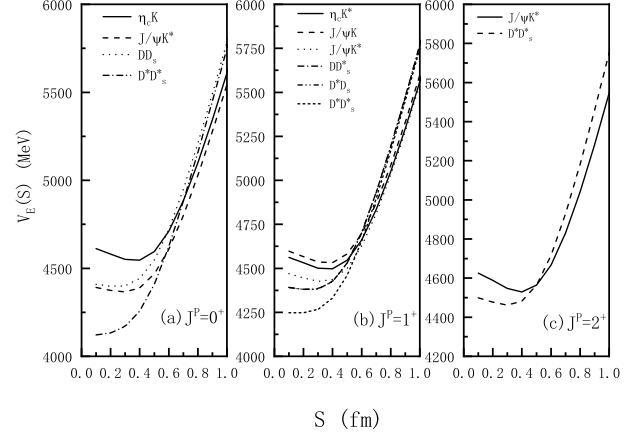
don't work between $c\bar{c}$ and $s\bar{u}$. Therefore, there is no any term which provides attractive interaction between two color singlet clusters in ChQM, which leads to absence of bound states in this system. In QDCSM, although the quark delocalization is largely weakened because of the heavy quarks in the system, it still affects the kinetic energy, which provides attractive interactions. The other interaction terms are also affected by the quark delocalization and provide repulsive interaction to this system. That's why the total effective potentials are possible to be attractive in QDCSM, although it is still difficult to form any bound state.

B. Diquark-antidiquark structure

With regards to the diquark-antidiquark structure, the results of both ChQM and QDCSM are listed in Tables IV. As shown in the table, the diquark-antidiquark structure has higher energy than the meson-meson structure so there is no any bound state. Besides, the energies in QDCSM are generally lower than that in ChQM. Since the color symmetry of the diquark and antidiquark are color octet, the color screening will make the quark delocalization work in QDCSM, which leads to lower energy in this model. We also find that the channel coupling of the diquark-antidiquark structure makes the energy a little lower, but the energy of each state is still higher than the corresponding threshold. However, since the confinement potential requires that the colorful subclusters diquark and antidiquark cannot fall apart directly,

TABLE IV: The energies (in MeV) of $c\bar{s}\bar{u}$ systems with the diquark-antidiquark structure in the ChQM and QDCSM.

		ChQM				QDCSM		
IJ^P	$[\chi^{\sigma_i}\chi^{f_j}\chi^{c_k}]$	E_{th}	E_{sc}	E_{cc1}	E_{cc2}	E_{sc}	E_{cc1}	E_{cc2}
$\frac{1}{2}0^+$	$\chi_{00}^{\sigma 1}\chi_d^{f 1}\chi_d^{c 1}$	3478.2	4462.3	4161.1	3964.6	4224.1	4034.3	3916.5
	$\chi_{00}^{\sigma 2}\chi_d^{f 1}\chi_d^{c 1}$		4171.6			4041.3		
	$\chi_{00}^{\sigma 1}\chi_d^{f 1}\chi_d^{c 2}$		4263.3			4146.6		
	$\chi_{00}^{\sigma 2}\chi_d^{f 1}\chi_d^{c 2}$		4350.1			4178.5		
$\frac{1}{2}1^+$	$\chi_{11}^{\sigma 3}\chi_d^{f 1}\chi_d^{c 1}$	3591.1	4426.8	4245.0	4091.2	4205.3	4089.2	4008.8
	$\chi_{11}^{\sigma 4}\chi_d^{f 1}\chi_d^{c 1}$		4426.3			4205.0		
	$\chi_{11}^{\sigma 5}\chi_d^{f 1}\chi_d^{c 1}$		4285.7			4116.3		
	$\chi_{11}^{\sigma 3}\chi_d^{f 1}\chi_d^{c 2}$		4334.2			4188.3		
	$\chi_{11}^{\sigma 4}\chi_d^{f 1}\chi_d^{c 2}$		4335.2			4188.8		
	$\chi_{11}^{\sigma 5}\chi_d^{f 1}\chi_d^{c 2}$		4379.1			4203.6		
$\frac{1}{2}2^+$	$\chi_{11}^{\sigma 6}\chi_d^{f 1}\chi_d^{c 1}$	3988.1	4486.5		4418.1	4251.7		4246.8
	$\chi_{11}^{\sigma 6}\chi_d^{f 1}\chi_d^{c 2}$		4431.1			4251.8		

FIG. 2: The effective potentials of the color singlet channels for the meson-meson $c\bar{s}\bar{u}$ systems in QDCSM.FIG. 3: The effective potentials of the hidden-color channels for the meson-meson $c\bar{s}\bar{u}$ systems in ChQM.

resonance states are possible in this configuration. We perform an adiabatic calculation to determine the possibility of the existence of any resonance state, the results of which are shown in Fig. 5.

Obviously, in both ChQM and QDCSM, the energy of each single channel will rise when the two subclusters are too close, so there is a hinderance for the state changing structure to meson-meson even if the energy of the diquark-antidiquark state is higher than the meson-meson state. So it is possible to form a resonance state. The minimum energy of each channel appears at the separation of $0.3 \sim 0.4$ fm in ChQM, the one appears at the separation of $0.6 \sim 0.7$ fm in QDCSM, which indicates that the diquark and antidiquark subclusters are close to

each other in both two models. Therefore, the resonance state may be the compact resonance state. According to the Table IV, after the channel coupling calculation, the lowest resonance energies in ChQM are 3964.6 MeV for $IJ^P = \frac{1}{2}0^+$, 4091.2 MeV for $IJ^P = \frac{1}{2}1^+$, 4418.1 MeV for $IJ^P = \frac{1}{2}2^+$; and those in QDCSM are 3916.5 MeV for $IJ^P = \frac{1}{2}0^+$, 4008.8 MeV for $IJ^P = \frac{1}{2}1^+$, and 4246.8 MeV for $IJ^P = \frac{1}{2}2^+$. By comparing the mass of the observed $Z_{cs}(3985)^-$, this Z_{cs} state is possible to be explained as a compact resonance state $c\bar{s}\bar{u}$ with $IJ^P = \frac{1}{2}0^+$ or $IJ^P = \frac{1}{2}1^+$. However, the scattering process of the corresponding open channels should be studied to confirm if there is any resonance state or not.

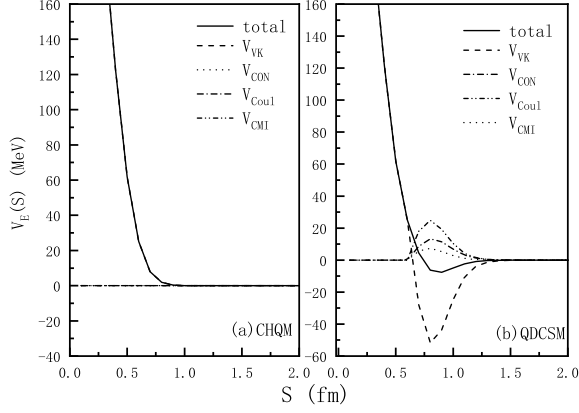


FIG. 4: The contributions to the effective potential of the $IJ^P = 00^+ \eta_c K$ channel from various terms of interactions in the ChQM and QDCSM.

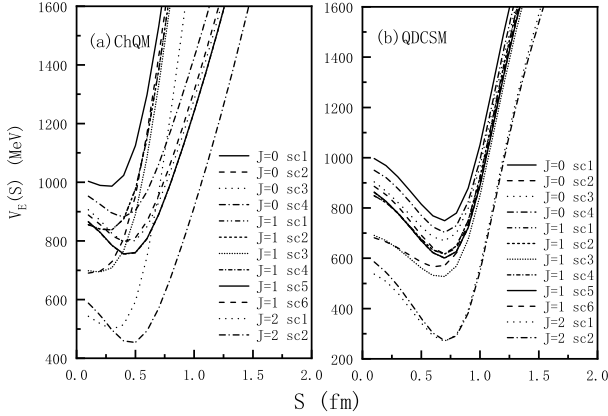


FIG. 5: The effective potentials for the diquark-antidiquark $cs\bar{c}u$ systems in two quark models.

IV. SUMMARY

In this work, we systematically investigate the low-lying charged hidden-charm tetraquark systems with

strangeness in two quark models ChQM and QDCSM. Two configurations, meson-meson and diquark-antidiquark, are considered. The dynamical bound-state calculation is carried out to search for any bound state in the $cs\bar{c}u$ systems. To investigate the effect of the channel coupling, both the single channel and the channel coupling calculation are performed. Meanwhile, an adiabatic calculation of the effective potentials is added to study the interactions of the systems and to find any resonance state.

The results are similar in both two quark models. The bound-state calculation shows that there is no any bound state in either ChQM or QDCSM, which excludes the reported $Z_{cs}(3985)^-$ as a molecular state $D_s D^*/D_s^* D/D_s^* D^*$. The study of the interaction between two mesons shows that the confinement interaction, the Coulomb interaction and the color-magnetic interaction don't work between two mesons of the $cs\bar{c}u$ systems, because there is no exchange terms between them. So it is difficult to obtain a molecular state in this $cs\bar{c}u$ system in present work. However, the effective potentials for the diquark-antidiquark $cs\bar{c}u$ systems shows the possibility of some resonance states with mass of $3916.5 \sim 3964.6$ MeV for $IJ^P = \frac{1}{2}0^+$, $4008.8 \sim 4091.2$ MeV for $IJ^P = \frac{1}{2}1^+$, $4246.8 \sim 4418.1$ MeV for $IJ^P = \frac{1}{2}2^+$. The newly reported Z_{cs} state is possible to be explained as a compact resonance state $cs\bar{c}u$ with $IJ^P = \frac{1}{2}0^+$ or $IJ^P = \frac{1}{2}1^+$. To confirm this conclusion, the scattering process of the corresponding open channels is needed, and the decay width can also be obtained by the scattering cross section, which is our further work.

Acknowledgments

This work is supported partly by the National Science Foundation of China under Contract Nos. 11675080, 11775118 and 11535005.

[1] M. Ablikim *et al.* [BESIII], Phys. Rev. Lett. **110**, 252001 (2013).
 [2] Z. Q. Liu *et al.* [Belle], Phys. Rev. Lett. **110**, 252002 (2013).
 [3] Z. Liu, [arXiv:1311.0762 [hep-ex]].
 [4] T. Xiao, S. Dobbs, A. Tomaradze and K. K. Seth, Phys. Lett. B **727**, 366-370 (2013).
 [5] J. M. Dias, F. S. Navarra, M. Nielsen and C. M. Zanetti, Phys. Rev. D **88**, 016004 (2013).
 [6] Z. G. Wang and T. Huang, Phys. Rev. D **89**, 054019

(2014).
 [7] C. Deng, J. Ping and F. Wang, Phys. Rev. D **90**, 054009 (2014).
 [8] S. S. Agaev, K. Azizi and H. Sundu, Phys. Rev. D **93**, 074002 (2016).
 [9] C. Liu, L. Liu and K. L. Zhang, Phys. Rev. D **101**, no.5, 054502 (2020).
 [10] H. X. Chen and W. Chen, Phys. Rev. D **99**, 074022 (2019).
 [11] E. Wilbring, H. W. Hammer and U. G. Meiner, Phys.

- Lett. B **726**, 326-329 (2013).
- [12] Y. Dong, A. Faessler, T. Gutsche and V. E. Lyubovitskij, Phys. Rev. D **88**, 014030 (2013).
 - [13] T. Gutsche, M. Kesenheimer and V. E. Lyubovitskij, Phys. Rev. D **90**, 094013 (2014).
 - [14] D. Y. Chen and Y. B. Dong, Phys. Rev. D **93**, 014003 (2016).
 - [15] A. Esposito, A. L. Guerrieri and A. Pilloni, Phys. Lett. B **746**, 194-201 (2015).
 - [16] Q. R. Gong, Z. H. Guo, C. Meng, G. Y. Tang, Y. F. Wang and H. Q. Zheng, Phys. Rev. D **94**, 114019 (2016).
 - [17] H. W. Ke and X. Q. Li, Eur. Phys. J. C **76**, 334 (2016).
 - [18] E. S. Swanson, Phys. Rev. D **91**, no.3, 034009 (2015).
 - [19] Y. Ikeda *et al.* [HAL QCD], Phys. Rev. Lett. **117**, no.24, 242001 (2016).
 - [20] S. Prelovsek and L. Leskovec, Phys. Lett. B **727**, 172-176 (2013).
 - [21] S. Prelovsek, L. Leskovec and D. Mohler, [arXiv:1310.8127 [hep-lat]].
 - [22] Y. Chen, M. Gong, Y. H. Lei, N. Li, J. Liang, C. Liu, H. Liu, J. L. Liu, L. Liu, Y. F. Liu, Y. B. Liu, Z. Liu, J. P. Ma, Z. L. Wang, Y. B. Yang and J. B. Zhang, Phys. Rev. D **89**, no.9, 094506 (2014).
 - [23] S. Prelovsek, C. B. Lang, L. Leskovec and D. Mohler, Phys. Rev. D **91**, no.1, 014504 (2015).
 - [24] M. Ablikim *et al.* [BESIII], [arXiv:2011.07855 [hep-ex]].
 - [25] M. Ablikim *et al.* [BESIII], Phys. Rev. Lett. **112**, no.2, 022001 (2014).
 - [26] J. Z. Wang, Q. S. Zhou, X. Liu and T. Matsuki, [arXiv:2011.08628 [hep-ph]].
 - [27] L. Meng, B. Wang and S. L. Zhu, [arXiv:2011.08656 [hep-ph]].
 - [28] M. Z. Liu, J. X. Lu, T. W. Wu, J. J. Xie and L. S. Geng, [arXiv:2011.08720 [hep-ph]].
 - [29] Z. Yang, X. Cao, F. K. Guo, J. Nieves and M. P. Valderrama, [arXiv:2011.08725 [hep-ph]].
 - [30] R. Chen and Q. Huang, [arXiv:2011.09156 [hep-ph]].
 - [31] M. C. Du, Q. Wang and Q. Zhao, [arXiv:2011.09225 [hep-ph]].
 - [32] X. Cao, J. P. Dai and Z. Yang, [arXiv:2011.09244 [hep-ph]].
 - [33] Z. F. Sun and C. W. Xiao, [arXiv:2011.09404 [hep-ph]].
 - [34] G. Rossi and G. Veneziano, [arXiv:2011.09774 [hep-ph]].
 - [35] Q. N. Wang, W. Chen and H. X. Chen, [arXiv:2011.10495 [hep-ph]].
 - [36] S. H. Lee, M. Nielsen, and U. Wiedner, J. Korean Phys. Soc. **55**, 424 (2009), arXiv:0803.1168 [hep-ph].
 - [37] M. B. Voloshin, Phys. Lett. B **798**, 135022 (2019), arXiv:1901.01936 [hep-ph].
 - [38] J. Ferretti and E. Santopinto, JHEP **04**, 119 (2020), arXiv:2001.01067 [hep-ph].
 - [39] D. Ebert, R. N. Faustov and V. O. Galkin, Phys. Lett. B **634**, 214-219 (2006).
 - [40] D. Y. Chen, X. Liu and T. Matsuki, Phys. Rev. Lett. **110**, 232001 (2013).
 - [41] A. Valcarce, H. Garcilazo, F. Fernández and P. Gonzalez, Rep. Prog. Phys. **68**, 965 (2005).
 - [42] F. Wang, G. h. Wu, L. j. Teng and J. T. Goldman, Phys. Rev. Lett. **69**, 2901 (1992).
 - [43] L. Z. Chen, H. R. Pang, H. X. Huang, J. L. Ping and F. Wang, Phys. Rev. C **76**, 014001 (2007).
 - [44] M. Chen, H. X. Huang, J. L. Ping and F. Wang, Phys. Rev. C **83**, 015202 (2011).
 - [45] X. Jin, Y. Xue, H. Huang and J. Ping, [arXiv:2006.13745 [hep-ph]].
 - [46] R. Aaij *et al.* [LHCb], Sci. Bull. **2020**, 65 doi:10.1016/j.scib.2020.08.032
 - [47] J. Vijande, F. Fernandez and A. Valcarce, J. Phys. G **31**, 481 (2005).
 - [48] M. Kamimura, Suppl. Prog. Theor. Phys. **62**, 236 (1977).
 - [49] H. Huang, P. Xu, J. Ping and F. Wang, Phys. Rev. C **84**, 064001 (2011).